Magnetodielectric effect and phonon properties of compressively strained $EuTiO_3$ thin films deposited on $(001)(LaAlO_3)_{0.29}$-$(SrAl_{1/2}Ta_{1/2}O_3)_{0.71}$

S. Kamba,[1,*] V. Goian,[1] M. Orlita,[2] D. Nuzhnyy,[1] J. H. Lee,[3] D. G. Schlom,[3,4] K. Z. Rushchanskii,[5] M. Ležaić,[5] T. Birol,[6] C. J. Fennie,[6] P. Gemeiner,[7] B. Dkhil,[7] V. Bovtun,[1] M. Kempa,[1] J. Hlinka,[1] and J. Petzelt[1]

[1]*Institute of Physics ASCR, Na Slovance 2, 182 21 Prague 8, Czech Republic*

[2]*Laboratoire National des Champs Magnétiques Intenses, CNRS-UJF-UPS-INSA, 25, avenue des Martyrs, 38042 Grenoble, France*

[3]*Department of Materials Science and Engineering, Cornell University, Ithaca, New York, 14853-1501, USA*

[4]*Kavli Institute at Cornell for Nanoscale Science, Ithaca, New York 14853, USA*

[5]*Peter Grünberg Institut, Quanten-Theorie der Materialien, Forschungszentrum Jülich GmbH, 52425 Juelich and JARA FIT, Germany*

[6]*School of Applied and Engineering Physics, Cornell University, Ithaca, New York, 14853, USA*

[7]*Laboratoire Structures, Propriétés et Modélisation des Solides, UMR8580 CNRS-Ecole Centrale Paris, 92295 Châtenay-Malabry Cedex, France*

(Received 6 January 2012; revised manuscript received 1 March 2012; published 30 March 2012)

Compressively strained epitaxial (001) $EuTiO_3$ thin films of tetragonal symmetry have been deposited on (001) $(LaAlO_3)_{0.29}$-$(SrAl_{1/2}Ta_{1/2}O_3)_{0.71}$ (LSAT) substrates by reactive molecular-beam epitaxy. Enhancement of the Néel temperature by 1 K with 0.9% compressive strain was revealed. The polar phonons of the films have been investigated as a function of temperature and magnetic field by means of infrared reflectance spectroscopy. All three in-plane polarized infrared active phonons show strongly stiffened frequencies compared to bulk $EuTiO_3$ in accordance with first-principles calculations. The phonon frequencies exhibit gradual softening on cooling, leading to an increase in static permittivity. Additional polar phonon with frequency near the TO1 soft mode was detected below 150 K. This mode coupled with the TO1 mode was assigned as the optical phonon from the Brillouin zone edge, which is activated in infrared spectra due to an antiferrodistortive phase transition and due to simultaneous presence of polar and/or magnetic nanoclusters. In the antiferromagnetic phase, we have observed a remarkable softening of the lowest-frequency polar phonon under an applied magnetic field, which qualitatively agrees with first-principles calculations. This demonstrates the strong spin-phonon coupling in $EuTiO_3$, which is responsible for the pronounced dependence of its static permittivity on magnetic field in the antiferromagnetic phase.

DOI: 10.1103/PhysRevB.85.094435 PACS number(s): 75.80.+q, 78.30.−j, 63.20.−e

I. INTRODUCTION

Multiferroic compounds in which magnetic and electric orders coexist are intensively studied due to their high potential in magnetoelectric devices as well as due to their rich and fascinating physics related to the magnetoelectric effect. Unfortunately, it appears that there are only few multiferroics in the nature, and their absolute majority exhibits multiferroic properties deeply below room temperature.[1] Moreover, most multiferroics exhibit antiferromagnetic (AFM) order and therefore only weak magnetoelectric coupling.[1] For this reason, there is an intensive search for new materials with ferromagnetic and ferroelectric order, where the magnetoelectric coupling could be high.

Fennie and Rabe[2] suggested a new route for preparation of multiferroics with a strong magnetoelectric coupling. They proposed to use a biaxial strain in the thin films for induction of the ferroelectric and ferromagnetic states in materials which are in the bulk form paraelectric and AFM. A basic condition for such a material is the strong spin-phonon coupling. Fennie and Rabe[2] proposed, based on their first-principles calculations, to use $EuTiO_3$ for such a purpose. Recently, Lee *et al.*[3] actually confirmed the theoretical prediction and revealed ferroelectric and ferromagnetic order in the tensile-strained $EuTiO_3$ thin films deposited on $DyScO_3$ substrates.

Bulk $EuTiO_3$ is an antiferromagnet with G-type AFM order below $T_N = 5.3$ K.[4] Temperature dependence of its permittivity ε' exhibits quantum paraelectric behavior, i.e., ε' increases on cooling and saturates at low temperatures due to quantum fluctuations, which inhibit the creation of long-range ferroelectric order. Recently, it was theoretically predicted that $EuTiO_3$ has an antiferrodistorted ground state.[5,6] Experimental studies show that, at room temperature, the crystal structure is cubic $Pm\bar{3}m$ perovskite,[7] which transforms to tetragonal $I4/mcm$ structure near 280 K.[8–10] ε'(T) exhibits a sharp drop below T_N due to a strong spin-phonon coupling.[11] A large interaction of the magnetic moment with the crystal lattice was also manifested by 7% increase of ε' with magnetic field, observed at 2 K.[11] Even though linear magnetoelectric coupling is forbidden by the symmetry of $EuTiO_3$, a strong biquadratic magnetoelectric coupling was recently reported below T_N.[12]

Low-temperature infrared (IR) reflectivity studies of $EuTiO_3$ ceramics reveal three polar phonons typical for cubic perovskites.[13,14] The frequency of the lowest-frequency (TO1) phonon decreases (the mode softens) on cooling, which fully explains the increase of static permittivity on lowering temperature via the Lyddane-Sachs-Teller (LST) relation. Below ≈100 K, the soft TO1 mode frequency deviates from the classical Cochran law and finally levels off below 30 K.[13] Such temperature dependence follows the Barrett formula,

which describes the saturation of ε'(T) at low temperatures due to quantum fluctuations. Based on the plasma frequencies of the polar phonons, the TO1 mode was assigned to Slater mode, i.e., Ti cations vibration against the oxygen octahedra, and the TO2 phonon (near 150 cm^{-1}) was assigned to Last mode, i.e., vibration of Eu cations against the TiO_6 octahedra.[14] Temperature dependence of the IR spectra indicated coupling (mixing of their eigenvectors) of both the modes.[14] Moreover, a strong spin coupling with the soft mode (SM) is expected microscopically due to a superexchange between Eu^{2+} $4f$ spins via the $3d$ states of the Ti^{4+} ions.[15]

Here, we report a study of the epitaxial compressively strained $EuTiO_3$ thin films deposited on (001) $(LaAlO_3)_{0.29}$-$(SrAl_{1/2}Ta_{1/2}O_3)_{0.71}$ (LSAT) substrate. Lee *et al.*[3] have shown that the maximum expected compressive strain of -0.9% in this case is not sufficient for induction of the ferroelectric and ferromagnetic order. Nevertheless, we will show here that the phonon properties of $EuTiO_3$/LSAT are strongly influenced by strain: The in-plane soft-mode frequency is significantly stiffened in comparison to the bulk $EuTiO_3$ ceramics and, moreover, its IR reflection band is more than five times narrower. It enabled us a detailed investigation of the magnetic field dependence of this phonon. We will show that shift of the lowest-frequency optical phonon with magnetic field is mainly responsible for observed magnetodielectric effect in $EuTiO_3$. Moreover, we will report about an antiferrodistortive (AFD) phase transition appearing in this film near 150 K.

II. EXPERIMENT

Films of two thicknesses (22 and 42 nm) were deposited by reactive molecular-beam epitaxy on the (001) LSAT substrate. Details of the deposition were described elsewhere.[16] The 42-nm film was slightly relaxed, but the 22-nm film was fully (-0.9%) compressively strained, its x-ray diffraction (XRD) showing the same in-plane lattice parameter (3.870 Å) as the substrate. The substrates of $10 \times 10 \times 1$ mm^3 size were provided by Uecker and his colleagues from the Institute of Crystal Growth, Berlin, Germany.

The unpolarized IR reflectance spectra were taken using a Bruker IFS 113v FTIR spectrometer at temperatures from 1.8 to 300 K with the resolution of 2 cm^{-1}. We checked also the polarized spectra at 300 and 10 K, but no in-plane anisotropy was observed, confirming that the substrate plate as well as the thin films are macroscopically optically isotropic in the (001) plane down to 10 K. An Optistat CF cryostat (Oxford Instruments) was used for cooling the samples without magnetic field down to 5 K. The investigated spectral range (up to 650 cm^{-1}) was limited by the transparency region of the polyethylene windows of the cryostat. A helium-cooled Si bolometer operating at 1.6 K was used as a detector. Custom-made superconducting magnetic cryostat was used for IR studies at various magnetic fields up to 13 T at temperatures between 1.8 and 4.2 K.

Each of the reflectance spectra was evaluated as a two-layer optical system.[17] At first, the bare substrate reflectivity was measured as a function of temperature and carefully fitted using the generalized factorized damped harmonic oscillator model[18]

$$\varepsilon^*(\omega) = \varepsilon_\infty \prod_{j=1}^{n} \frac{\omega_{\mathrm{LO}j}^2 - \omega^2 + i\omega\gamma_{\mathrm{LO}j}}{\omega_{\mathrm{TO}j}^2 - \omega^2 + i\omega\gamma_{\mathrm{TO}j}}, \tag{1}$$

where $\omega_{\mathrm{TO}j}$ and $\omega_{\mathrm{LO}j}$ denote the transverse and longitudinal frequency of the jth polar phonon, respectively, and $\gamma_{\mathrm{TO}j}$ and $\gamma_{\mathrm{LO}j}$ denote their corresponding damping constants. $\varepsilon^*(\omega)$ is related to the reflectivity $R(\omega)$ of the bulk substrate by

$$R(\omega) = \left| \frac{\sqrt{\varepsilon^*(\omega)} - 1}{\sqrt{\varepsilon^*(\omega)} + 1} \right|^2. \tag{2}$$

The high-frequency permittivity $\varepsilon_\infty = 5.88$ resulting from the electronic absorption processes was obtained from the room-temperature frequency-independent reflectivity tails above the phonon frequencies and was assumed to be temperature independent.

When analyzing the reflectance of the substrate together with the film, we kept the earlier fitted bare substrate parameters fixed at each temperature and adjusted only the dielectric function of the film. For this purpose, we preferentially used a classical three-parameter damped oscillator model[18]

$$\varepsilon^*(\omega) = \varepsilon_\infty + \sum_{j=1}^{n} \frac{\Delta\varepsilon_j \omega_{\mathrm{TO}j}^2}{\omega_{\mathrm{TO}j}^2 - \omega^2 + \mathrm{i}\omega\gamma_{\mathrm{TO}j}} \tag{3}$$

since it uses fewer fitting parameters ($\Delta\varepsilon_j$ marks dielectric strength). This approach is well justified because the damping of LO phonons of the film does not influence appreciably the reflectance spectra. Only the line shape of the lowest-frequency doublet was not well reproduced and therefore a coupled damped harmonic model was applied at low temperatures (see the following).

The IR reflectance measurements were performed on samples with a substrate of 1-mm thickness, which was thick enough to avoid the parasitic IR signal from the multiple reflection in the substrate. The same samples were afterward polished to $248 \pm 1\mu$m to reach the optimal microwave (MW) resonance near 15 GHz where the samples were measured as the composite $TE_{01\delta}$ dielectric resonators in the shielding cavity[19] using their dielectric resonance. Precisely the same thicknesses of bare substrates and substrates with the films are needed for an accurate evaluation of the in-plane complex permittivity of the films. Each sample was measured twice, in the Sigma System M18 temperature chamber (100–370 K) and in the He-cooled Janis close-cycle cryostat (10–370 K).

High resolution x-ray diffraction measurements were performed on a two-axis diffractometer in a Bragg-Brentano geometry (focalization circle with a diameter of 50 cm). Cu-Kα (wavelength $\lambda = 1.54056$ Å) radiation was emitted from a 18-kW rotating anode generator. The out-of-plane lattice constant of the film as well as that of the substrate were determined with accuracy of ± 0.0003 Å. The cryostat was operating between 10 and 300 K with an accuracy better than 0.5 K. Magnetic properties were measured using a SQUID magnetometer (Quantum Design) from 2 to 30 K. The sample with the 42-nm thin film was cut to four pieces of $3.5 \times 4.5 \times 0.248$ mm^3 size, and all four stacked samples were measured simultaneously.

TABLE I. Polar phonon frequencies in cm^{-1} of $EuTiO_3$ from the first principles for the bulk and for films on two different substrates $SrTiO_3$ (i.e., no strain) and LSAT (compressive strain −0.9%). Experimental results obtained on 22 nm thick film are given in the last column for comparison. Only the lowest-frequency phonon was studied as dependent on magnetic field. The calculations are valid at 0 K. If the oxygen octahedron rotations *are not* taken into account, the structure of the bulk $EuTiO_3$ is $Pm\bar{3}m$. If the oxygen octahedron rotations *are* taken into account, the space group is $I4/mcm$, the same both in bulk and compressively strained thin films. The in-plane polarized polar modes have the E_u symmetry, whereas the out-of-plane modes have the A_{2u} symmetry.

Bulk $EuTiO_3$ $Pm\bar{3}m$		Bulk $EuTiO_3$ $I4/mcm$				$EuTiO_3/SrTiO_3$ $I4/mcm$				$EuTiO_3$/LSAT $I4/mcm$				$EuTiO_3$/LSAT Experiment at 1.9 K	
F_{1u}		A_{2u}		E_u		A_{2u}		E_u		A_{2u}		E_u		E_u	
FM	AFM	FM	AFM	FM	AFM	FM	AFM	FM	AFM	FM	AFM	FM	AFM	FM	AFM
70	77	125	133	107	113	132	138	77	86	113	124	121	125	104.0, ?	105.5, 115
162	165	158	159	156	158	159	161	147	148	160	161	164	166	?	162
				251	251			246	246			255	255		
				422	422			414	414			428	428		
549	550	533	534	526	527	536	537	519	519	531	532	532	532	?	551

III. THEORETICAL CONSIDERATIONS

In parallel with the experimental studies, we also investigated the $EuTiO_3$ films using a first-principles density functional (DFT) calculation within the spin-polarized generalized gradient approximation (GGA). In particular, we have studied the effect of the strain and magnetic field on phonon frequencies in the bulk and thin films. Our initial guess for the low-temperature structure of $EuTiO_3$ is analogous to that of the bulk $SrTiO_3$ ($I4/mcm$ space group). In the course of this work, this structure was confirmed experimentally[10] for the bulk $EuTiO_3$. Our first-principles calculations confirm this result.[20]

For the electronic-structure calculations and structural relaxations, we used projector augmented-wave potentials as implemented in the Vienna *ab initio* simulation package (VASP). To account for the strong electron correlation effects on the f shell of Eu atoms, we used the DFT+U scheme in the Dudarev's approach with an onsite Hubbard U and Hund's exchange J_H. For the bulk $EuTiO_3$ of space group $Pm\bar{3}m$, $U = 5.7$ eV is used. In order to correct for the effect of oxygen octahedron rotations on the magnetism, the Hubbard parameter is increased to $U = 6.2$ eV for $EuTiO_3$ in the space group $I4/mcm$.[20] Hund's exchange is kept fixed at $J_H = 1.0$ eV for all calculations. Details of the calculations can be found in Refs. 5 and 6.

For the sake of comparison with the experiment, we have calculated frequencies of the polar phonon modes in the bulk cubic and tetragonal $EuTiO_3$ as well as in tetragonal lattices with equatorial lattice parameters fixed to those of the $SrTiO_3$ and LSAT substrates. In order to estimate the frequency changes under strong bias magnetic field, the calculations were carried out both for the AFM order (anticipated ground state) and for ferromagnetic (FM) order (i.e., for the expected induced magnetic order under magnetic field). Resulting mode frequencies are listed in Table I.

IV. RESULTS

A. Magnetic properties

Magnetization curves taken at various external magnetic fields (see Fig. 1) reveal $T_N = 6.3$ K. It means that the −0.9% compressive strain in the film enhances T_N by 1.0 K because the coupling of spins localized at the 4f levels of Eu cations increases with the reducing lattice parameter in the compressively strained films. Note that the +1.1% tensile strain in $EuTiO_3/DyScO_3$ induces the ferromagnetic order below 4.2 K.[3] On the other hand, it was reported that the as-deposited thin $EuTiO_{2.86}$ films on $SrTiO_3$ (this substrate has exactly the same lattice constant 3.905 Å as the bulk $EuTiO_3$) exhibit an elongated c axis and a ferromagnetic order below 5 K,[21,22] while the same films post annealed at 1000 °C, in reducing atmosphere exhibit AFM order and relaxed out-of-plane lattice strain.[22]

B. Temperature dependence of the phonon spectra

IR reflectance of the $EuTiO_3$ 42-nm film plotted at various temperatures is shown in Fig. 2. Comparison of the spectra with those of bare LSAT substrate allows us to distinguish the three TO phonons of the film (marked by the arrows). The highest-frequency phonon is marked TO4 (the TO3 phonon is silent). The two lowest-frequency TO phonons show up softening on cooling, which is better seen in the inset of Fig. 2.

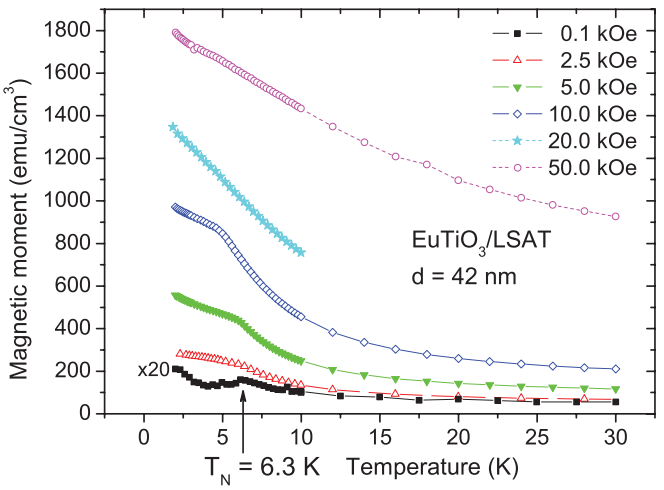

FIG. 1. (Color online) Temperature dependence of the magnetization of 42-nm-thick film at different external magnetic fields.

The three modes correspond well to the three polar modes of the cubic $EuTiO_3$, as shown in Table I. Moreover, a new weak mode appears near 112 cm^{-1} below 100 K. Since the 42-nm film was not fully strained, we have measured also the IR reflectance spectra from a fully (and uniformly) strained 22-nm film. Due to the smaller film thickness, the intensity of the TO1 reflection band is lower (see Fig. 3), but one can clearly see the mode splitting already below 150 K. Note that in this case the new mode is activated below the TO1 phonon frequency, while in the thicker film the new mode has higher frequency than the TO1 mode. Origin of the new mode will be discussed in Sec. V.

Shape of the IR reflectance bands in Fig. 3 is rather unusual, and the splitting of the TO1 mode can not be fitted well just with a sum of independent oscillators [Eq. (3)]. Therefore, the coupled oscillator formula was used for the fit of the split modes (their bare parameters are marked with subscripts a and b) and the rest of modes were fitted with Eq. (3). The coupled oscillator formula has the form[23]

$$\varepsilon^*(\omega) = \varepsilon_\infty + \frac{\Delta\varepsilon_{1a}\omega_{\mathrm{TO}1a}^2\left(\omega_{\mathrm{TO}1b}^2 - \omega^2 + \mathrm{i}\omega\gamma_{\mathrm{TO}1b}\right) + \Delta\varepsilon_{1b}\omega_{\mathrm{TO}1b}^2\left(\omega_{\mathrm{TO}1a}^2 - \omega^2 + \mathrm{i}\omega\gamma_{\mathrm{TO}1a}\right) - 2i\omega\Gamma\sqrt{\Delta\varepsilon_{1a}\omega_{\mathrm{TO}1a}^2\Delta\varepsilon_{1b}\omega_{\mathrm{TO}1b}^2}}{\left(\omega_{\mathrm{TO}1a}^2 - \omega^2 + \mathrm{i}\omega\gamma_{\mathrm{TO}1a}\right)\left(\omega_{\mathrm{TO}1b}^2 - \omega^2 + \mathrm{i}\omega\gamma_{\mathrm{TO}1b}\right) + \omega^2\Gamma^2} \tag{4}$$

using the imaginary coupling constant Γ model. The rest of the symbols have the same meaning as in Eq. (3).

Figure 4(a) shows the temperature evolution of the polar phonon frequencies below 170 cm^{-1} obtained from the reflectance fits of both films. At 10 K, the TO phonon frequencies are 83, 151, and 533 cm^{-1} for the bulk ceramics,[14] while our 22-nm film shows phonons at 115, 162, and 551 cm^{-1} and the additional new mode at 105 cm^{-1}. There is a strong phonon frequency stiffening in the films due to the compressive strain. Note also that the phonon frequencies are higher in the 22-nm film than in the 42-nm one [see Fig. 4(a)], obviously due to the higher strain in the former case.

Complex permittivity spectra evaluated from the IR reflectance are shown in Fig. 5. Stiffening of all in-plane polar phonons is responsible for a lower in-plane permittivity ε' in the films compared with the bulk sample. At 10 K the static permittivity reaches the value of 120 compared to 405 in the single crystal.[11] Here, it should be stressed that compressive strain reduces the in-plane permittivity, but the out-of-plane permittivity should be enhanced because the TO1 phonon component polarized perpendicularly to the film plane should be softer. Unfortunately, we can not see this phonon in our near-normal reflectivity geometry.

In our fit, we used $\Delta\varepsilon_{1a} = 0$, i.e., we suppose that the bare lowest-frequency mode has zero dielectric strength. The imaginary coupling does not shift the phonon frequencies, it merely deforms the spectral line shape and transfers the oscillator strength $\Delta\varepsilon\omega_{\mathrm{TO}}^2$ from TO1b to the new TO1a mode [see Fig. 4(b)]. Dramatic increase of the coupling constant Γ is seen on cooling below 150 K in inset of Fig. 5. This causes the increase of its strength on cooling. Also, the temperature dependences of the TO1b and TO2 mode oscillator strengths

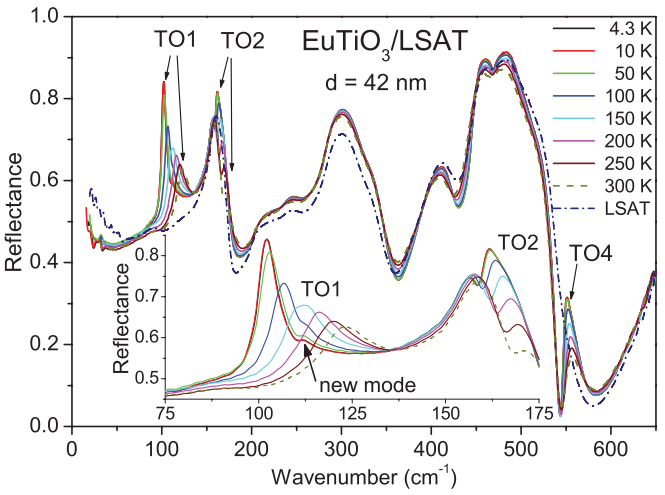

FIG. 2. (Color online) Temperature dependence of the IR reflectance of the $EuTiO_3$ 42-nm film deposited on the LSAT substrate. Room-temperature reflectivity of pure LSAT substrate is also plotted for comparison (dashed-dotted line). Phonons from the thin film are marked. Inset shows the enlarged low-frequency part of the reflectance spectra, where the softening of TO1 and TO2 phonons is clearly seen on cooling.

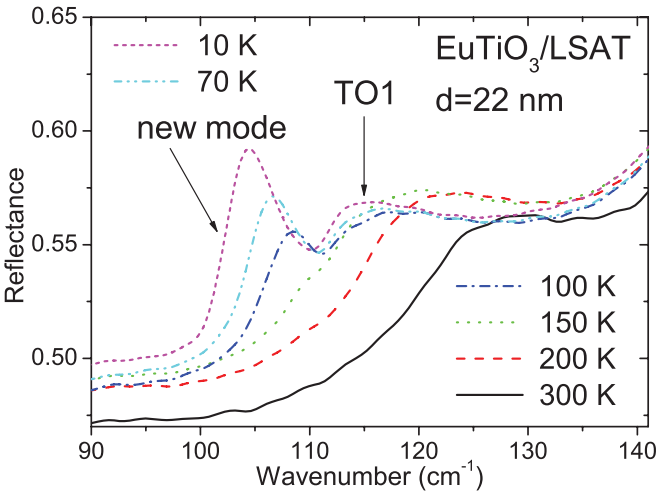

FIG. 3. (Color online) Temperature dependence of the low-frequency IR reflectance of fully strained $EuTiO_3$ 22-nm film deposited on a LSAT substrate. Remarkable TO1 phonon softening on cooling and activation of a new mode below 150 K is clearly seen.

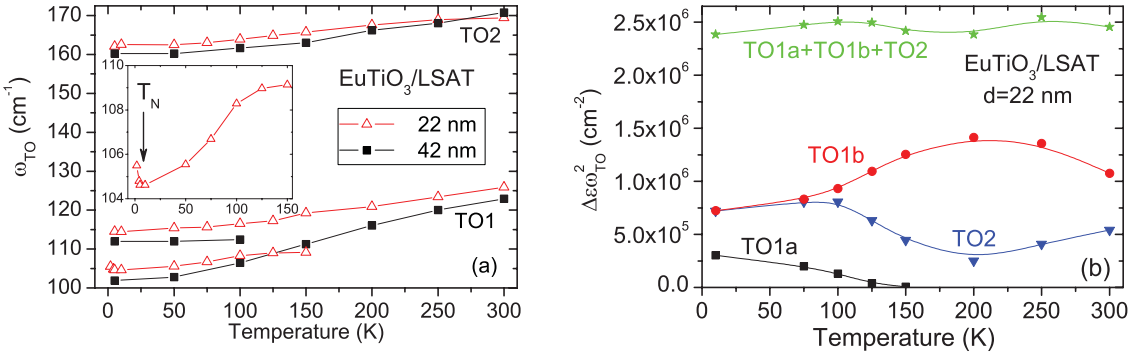

FIG. 4. (Color online) (a) Temperature dependence of the phonon frequencies for the $EuTiO_3$ films of two thicknesses 42 and 22 nm below 170 cm^{-1}. Stiffening of the TO1 and TO2 phonon frequencies in the more strained 22-nm film is seen. The new mode in the 22-nm film activates by 50 K higher than in the thicker film. The inset shows the temperature dependence of the new mode frequency in expanded scale down to 1.9 K. Mode hardening below the Néel temperature is clearly seen. (b) Temperature dependence of the oscillator strengths of all the modes seen below 200 cm^{-1}. One can see that the new TO1a mode gains strength from the TO1b mode. The sum of the oscillator strengths of all three modes remains constant within accuracy of the measurements, i.e., the sum rule (Ref. 13) is satisfied.

are remarkable. They give evidence on mixing of eigenvectors of both the modes.

C. Microwave dielectric measurements

The nonmonotonous dependence of the oscillator strengths of TO1b and TO2 modes [see Fig. 4(b)] could be related to an AFD phase transition involving antiphase tilts of the oxygen octahedra ($a^0a^0c^-$ in Glazer notation). This phase transition occurs in the bulk $EuTiO_3$ near room temperature,[8–10] but in the strained films it can be expected at lower temperatures (e.g., near 180 K in the 1% tensile strained $EuTiO_3/DyScO_3$).[3] Also, the TO1a-TO1b coupling could be related to this transition if the distorted phase would be ferroelectric. Therefore, we have investigated the temperature dependence of the in-plane MW permittivity of the film and of the substrate itself. Complex permittivity of the film measured near 15 GHz shows a dielectric anomaly near 120 K (see Fig. 6) reminding of a ferroelectric phase transition. Nevertheless, the second harmonic generation (SHG) measurements of the $EuTiO_3$/LSAT film did not reveal any acentric phase down to 2 K.[3] Moreover, from theory we know that the spontaneous polarization (and the main dielectric anomaly) should occur in the [001] direction in the compressively strained films,[2,24] whereas we measure only the in-plane dielectric response. It is suspicious that the low-temperature MW ε' is higher than the sum of phonon contributions to ε' (see Fig. 6) and that the maximum of ε' occurs 30 K below the temperature where the new mode activates in the IR spectra. Since we do not see any phonon

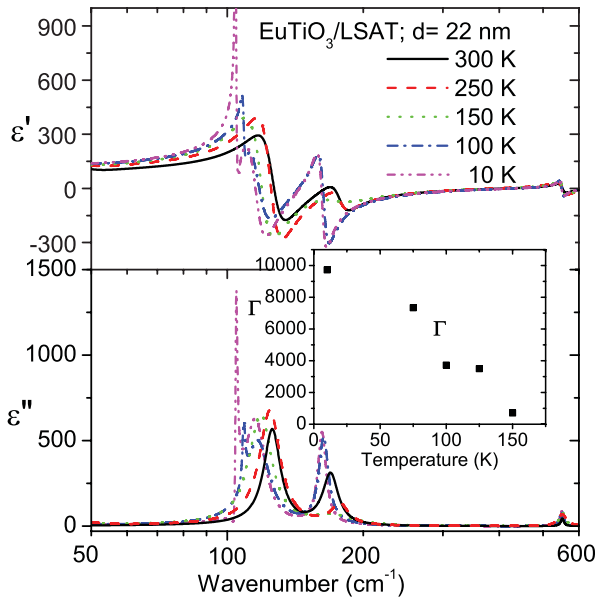

FIG. 5. (Color online) Complex dielectric function spectra of 22-nm $EuTiO_3$ film evaluated at various temperatures from the reflectance spectra in Fig. 3. The inset shows the temperature dependence of the imaginary coupling constant between two lowest-frequency modes.

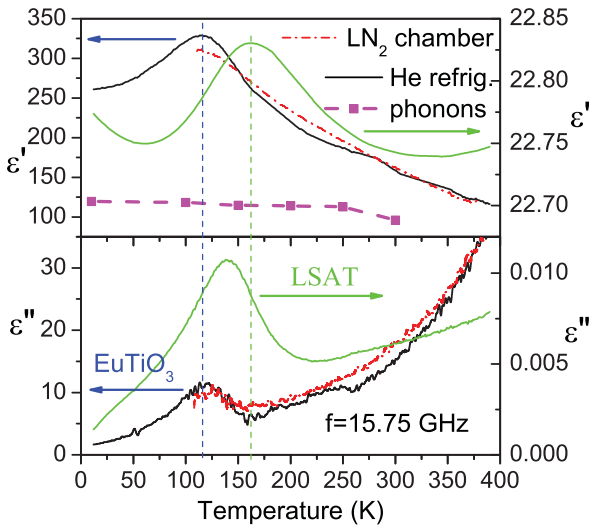

FIG. 6. (Color online) Temperature dependence of the complex permittivity in the 22-nm $EuTiO_3$ film (left scale) and the LSAT substrate (right scale) measured at 15.75 GHz. The thin-film MW data were obtained using two low-temperature devices (LN_2 chamber and He refrigerator). Static permittivity calculated from the phonon contributions (solid dots) is shown for comparison.

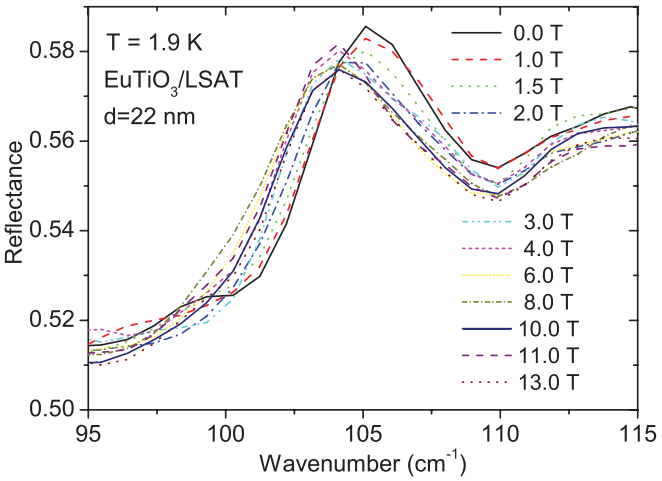

FIG. 7. (Color online) IR reflectance spectra of the 22-nm thin film at 1.9 K taken at various magnetic fields. The shift of phonon frequency is clearly seen.

anomaly in the IR spectra explaining the dielectric anomaly near 120 K, it seems that the MW dielectric anomaly has its origin in some dielectric dispersion below the phonon frequencies, most probably due to diffusion of charged defects (e.g., oxygen vacancies). Such defects play the main role in the conductivity of the films, which deteriorates the dielectric studies of $EuTiO_3$/LSAT in the kHz region.

D. Magnetodielectric effect and tuning of the phonon frequency by magnetic field

Bulk $EuTiO_3$ has a high static $\varepsilon' \simeq 400$ and low SM frequency. Therefore, it shows a high (7%) tunability of ε' by the magnetic field B,[11] and an unusually high 7- cm^{-1} change of the SM TO1 frequency with B is expected theoretically.[2] Such a shift was not confirmed in our IR spectra of the bulk ceramics, presumably because the TO1 reflection band is too broad (almost 100 cm^{-1}).[13] However, the sharper TO1 reflectance band in compressively strained $EuTiO_3$ films (see Figs. 2 and 3) appears to be more promising for such observation, although the expected frequency shift (see Table I) is somewhat lower ($\approx$4 cm^{-1}).

Actually, we have observed an almost 2- cm^{-1} decrease of the lowest-frequency phonon with B up to 10 Tesla (see Figs. 7 and 8). The phonon frequency shifts could be determined with a high accuracy of 0.1 cm^{-1} thanks to the sharp feature of the reflectance band. The absolute changes of the phonon frequencies on B were similar and reproducible in both films, even though the origin of the sharp phonon seen in Figs. 2 and 3 appears to be different. It corresponds predominantly to TO1 and an optical phonon from the Brillouin zone edge (see the discussion in the next section) in the 42- and 22-nm films, respectively. The higher-frequency component of the TO1 reflectance band is weaker and broader, therefore, it is not possible to evaluate its change with B. The magnetodielectric effect, i.e., the relative change of the static permittivity with magnetic field B $[\Delta\varepsilon'(B)/\varepsilon'(0)]$ obtained from the fits of reflectance spectra, is plotted in Fig. 9. As expected, one can see that the change of $\Delta\varepsilon'(B)/\varepsilon'(0)$ in the thin film is almost three times smaller than that in the single crystal[11] because the

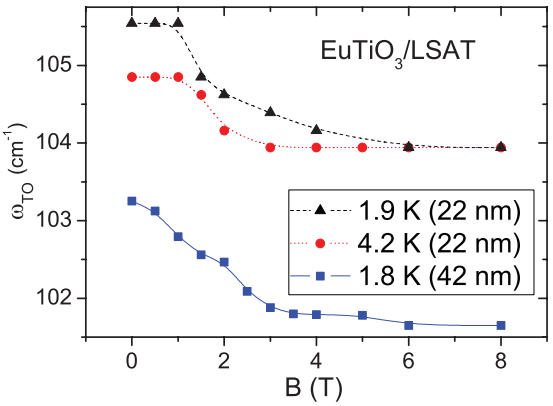

FIG. 8. (Color online) Magnetic field dependence of the lowest-frequency phonon obtained from the fits of the IR reflectance of both films at various temperatures below T_N.

phonons are stiffened in the films. The change of $\Delta\varepsilon'(B)/\varepsilon'(0)$ appears to be larger at 1.9 K than at 4.2 K (Fig. 9). It is caused by the larger phonon frequency shift with B at 1.9 K (see Fig. 8) since also the shift of the phonon frequency on cooling below T_N is larger at 1.9 K than at 4.2 K [see inset of Fig. 4(a)]. It corresponds also to larger relative change of the permittivity at 2 K than at 4.2 K reported in single crystal[11] and ceramics.[13] Here, it should be noted that the magnetic field influence on the A_{2u} SM component polarized perpendicular to the film plane (unattainable in our experiment) should be higher than the influence on the phonons polarized in the film plane. This is shown also in Table I.

Phonon frequencies obtained from the first-principles calculation in the AFM (i.e., without applied B) and in the ferromagnetic phase (i.e., in a high B) are summarized in Table I. One can see that mainly the lowest-frequency phonons shift down with the magnetic field. Theoretical frequency shift is twice larger in Table I than in our experiment (Fig. 8) because the calculations were performed at conditions of 0 K, while the experiment was done at $\approx$2 K and the shift should increase on cooling below T_N. In this way, we confirmed that the magnetodielectric effect in $EuTiO_3$ is due to the change of the polar phonon frequency with magnetic field.

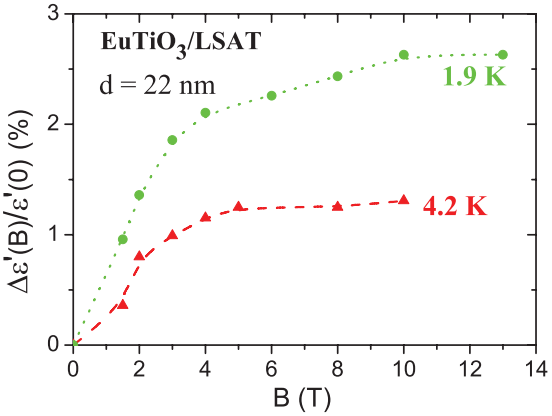

FIG. 9. (Color online) Magnetic field dependence of the relative changes of static permittivity obtained from the fits of IR reflectance of the 22-nm thin film.

It is well known from the literature that it is rather easy to change the phonon frequencies by hydrostatic pressure or external electric field. This effect is most remarkable in ferroelectrics, in which the ferroelectric SM is highly sensitive to boundary conditions. Electric field dependence of the ferroelectric SM was observed in Raman scattering of $SrTiO_3$,[25,26] and the hydrostatic pressure dependences of the SM were reviewed by Samara and Peercy.[27]

On the other hand, direct observations of phonon frequency changes on application of external magnetic field B are very scarce in literature and most of magnetic materials do not exhibit measurable effects. Ruf *et al.*[28] observed 1.5 cm^{-1} change of one phonon line with B in the Raman scattering spectra of $YBa_2Cu_3O_7$. This phonon frequency was sensitive to the superconductive phase transition and its changes were observed slightly below T_c under the field of 6–12 T. Sushkov *et al.*[29] reported on small B-dependent line-shape changes in the IR absorption spectra of molecular magnet Mn_{12} acetate, but a very high magnetic field of 30 T was necessary to get a measurable effect. Multiferroics exhibit relatively high tunability of ε' so that also larger changes of phonon frequencies with B could be expected. This was confirmed in $GdMnO_3$ and $DyMn_2O_5$ multiferroics.[30,31] In the former case, a phonon frequency change by less than 1 cm^{-1} was observed due to a phonon coupling with magnon,[30] while in the latter case a high field of 18 T was necessary to see a $\sim$2 cm^{-1} change of phonon frequency.[31] In our $EuTiO_3$ film, the phonon frequency change due to B is comparable to the previous case, but a much lower magnetic field was needed.

It should be stressed that the magnetodielectric effect in $EuTiO_3$ is not caused by a linear magnetoelectric coupling since bilinear terms $\alpha_{ij}H_iE_j$ (where H_i and E_j are components of the magnetic and electric fields, respectively) are not allowed in the thermodynamic potential.[12] Nevertheless, higher-order magnetoelectric effects, accounted for by the $\beta_{ijk}H_iH_jE_k$ and $\delta_{ijkl}H_iH_jE_kE_l$ terms in the thermodynamic potential, are permitted. The strong quadratic and biquadratic magnetoelectric effects were actually experimentally confirmed in bulk $EuTiO_3$ by Shvartsman *et al.*[12]

Dzyaloshinskii recently proposed a splitting of polar phonons in ferroelectrics due to an external magnetic field.[32] We do not see any splitting of phonons in the magnetic field, but we observe a 50% increase of the SM damping with magnetic field (see the broadening of reflection band with magnetic field in Fig. 7). At 1.9 K, its damping is 4.2 cm^{-1} at $B = 0$ T, while at $B = 13$ T, it is 6 cm^{-1}. Broadening of the phonon linewidth could be a consequence of a small phonon splitting, which is not resolved.

V. DISCUSSION

Let us now try to explain the origin of activation of the new mode near the TO1 phonon frequency in the IR spectra of $EuTiO_3$/LSAT (see Fig. 4). We consider two possibilities: (1) the doubly degenerate E_u component of the TO1 phonon probed in our experiment splits due to anisotropic in-plane strain, which is created due to a phase transition in the LSAT substrate. (2) The new mode originates from the Brillouin zone (BZ) edge due to an AFD phase transition (with multiplication of the primitive unit cell and BZ folding).

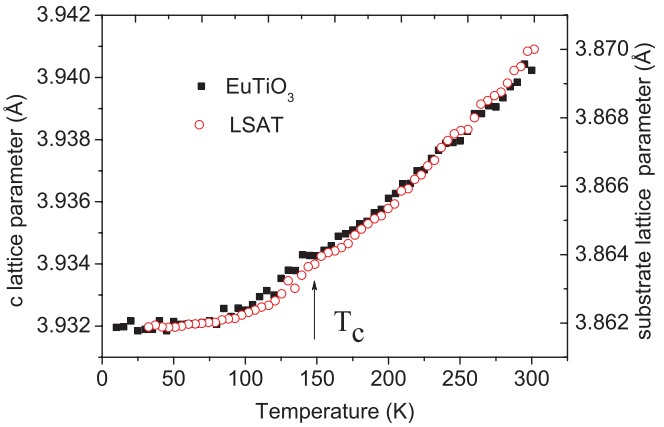

FIG. 10. (Color online) Temperature dependence of the out-of plane lattice parameter of the $EuTiO_3$ film (thickness 22 nm) and of the LSAT substrate.

Let us discuss the first possibility. The in-plane polarized modes can split if the tetragonal symmetry of film reduces to orthorhombic or lower-symmetry structure. It is possible only in the case when the in-plane strain would be anisotropic, i.e., the LSAT substrate would not be cubic. Indeed, it has been reported that the LSAT substrate exhibits a small distortion from cubic symmetry near 150 K and its low-temperature phase has tetragonal or orthorhombic symmetry.[35] We have measured temperature dependence of the LSAT lattice constant and it really exhibits a small hump near 150 K (see Fig. 10), and the same anomaly is revealed also in the out-of plane $EuTiO_3$ film lattice parameter. Moreover, the structural phase transition in LSAT can be recognized also in the MW dielectric permittivity, where a small anomaly was observed near 150 K (see Fig. 6). Nevertheless, in the case of substrate-induced anisotropic strain, the split modes should have different symmetries and therefore they can not couple, as observed in our spectra. Moreover, the possible anisotropic strain from the noncubic LSAT substrate should as well split the phonons in $SrTiO_3$/LSAT ($SrTiO_3$ and $EuTiO_3$ have the same lattice constant and therefore the strain in both films is the same), but this was not detected.[33] On the other hand, we have revealed the same new phonon activated in IR spectra near 150 K in $EuTiO_3$ films deposited on $NdGaO_3$ and $LaAlO_3$.[10] Compressive strains in both films are slightly relaxed and have the value of about 0.9%,[10] i.e., close to $EuTiO_3$/LSAT. Since the $NdGaO_3$ and $LaAlO_3$ substrates do not exhibit any structural phase transition, the new mode observed in all three films can not be activated due to anisotropic strain.

Let us discuss the second possibility that the new mode originates from the BZ edge. It can be expected that the AFD phase transition evidenced in the bulk $EuTiO_3$ (Refs. 8–10) and tensile strained thin-film $EuTiO_3/DyScO_3$ (see supplement of Ref. 3) should occur in the compressive thin films as well. The tetragonal $I4/mcm$ symmetry reported for the bulk can be also well compatible with the thin-film epitaxial geometry under compressive strain. Temperature of the phase transition may be considerably shifted in comparison to the bulk, of course. In the AFD phase, two new E_u phonons near 255 and 430 cm^{-1} stemming from the R point of the BZ edge become active in the IR spectra, as it can be seen from Table I.

However, the frequencies are much higher than that of our new mode seen between 110 and 105 cm^{-1}.

It is known that two structural soft modes (SMs) from the R point of the BZ edge can be activated in low-frequency Raman spectra below the AFD phase transition in $SrTiO_3$ ($T_C = 105$ K).[36] The AFD structure of $SrTiO_3$ is the same $I4/mcm$ as in $EuTiO_3$ and the two AFD SMs should be IR inactive in both materials, if their structure remains centrosymmetric. However, these AFD SMs were also discovered in the low-temperature IR spectra of bulk $SrTiO_3$ ceramics[37] and polycrystalline films.[38] Their activation was explained by polar distortion near the grain boundaries.[37,38] Activation of the AFD SM was also observed in tensile-strained $SrTiO_3$ and $EuTiO_3$ films on $DyScO_3$ substrates since the tensile strain induces a ferroelectricity in both films.[3,35,39] Our new mode seen near 105 cm^{-1} does not remind of any AFD SM because it does not harden below the assumed AFD transition temperature near 150 K. Nevertheless, it can be an optical mode from the BZ edge. Theoretical calculations[40] show that the lowest-frequency optical branch exhibits almost no q dispersion in BZ, therefore, the TO1 mode ($\mathbf{q} = 0$) and the optical mode from the BZ edge have almost the same frequency. AFD SMs have probably much lower frequencies, therefore they are not resolved in our spectra. Nevertheless, both AFD SMs and optical mode from the BZ boundary can be activated after folding of BZ zone only if the crystal structure becomes at least locally broken. Even if we know that the loss of the inversion center was not evidenced by the SHG signal in $EuTiO_3$/LSAT,[3] it is known that the IR probe is sensitive on local breaking of the symmetry known, e.g., from polar nanoclusters in relaxor ferroelectrics.[41]

Here, we propose a new possible mechanism of polar nanocluster appearance in the $EuTiO_3$ as the consequence of AFD phase transition and oxygen vacancies, which are always present in the lattice. Let us imagine that we have oxygen vacancies in the TiO_2 plane of the perovskite structure (see Fig. 11). Then, in the ideal perovskite structure without octahedra tilting, the local environment around the vacancy is antipolar: two neighboring Ti atoms are equally displaced in opposite directions. In a structure which allows oxygen octahedra tilting, the displacements of Ti atoms are antipolar in one direction, but with uncompensated dipoles in the orthogonal direction (see Fig. 11). In such a case, the local inversion symmetry is broken. We have calculated the structure in a 40-atomic simulation cell (i.e., $EuTiO_{2.875}$ instead of $EuTiO_3$) around this defect and found that it has caused Ti displacements not only around the vacancy, but also in other Ti's in the vacancy neighborhood. Of course, the displacements of the neighboring Ti are the largest. Also, we found that the formation energy of the O vacancy in the TiO_2 plane is 0.03 eV lower than the vacancy in the EuO plane (i.e., apical oxygen).

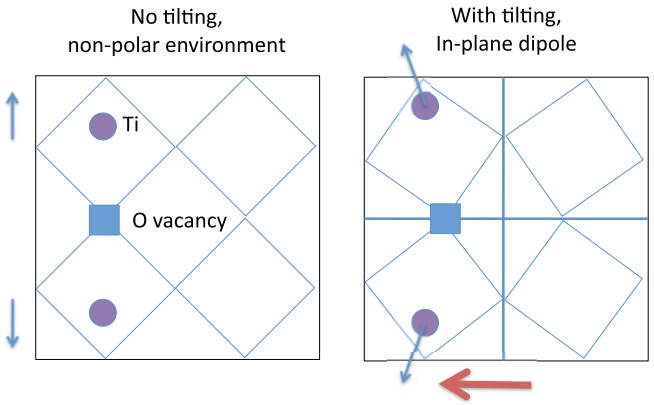

FIG. 11. (Color online) Schematic plot of the perovskite crystal structure in the view along [001] axis in the (a) untilted and (b) tilted AFD phases. Squares are marks for the oxygen octahedra, Eu cations are not shown. Orientation of the electric dipole moment created by the Ti displacement in the vicinity of oxygen vacancy in the tilted phase is marked by a large red arrow.

The IR inactive folded modes can become IR active also if we assume AFM short-range order even if it remains centrosymmetric. Our density functional calculations for an auxiliary $I\bar{4}2m$ structure compatible with AFM order yielded a new IR active phonon (originally optical one from the BZ edge) with frequency that is 12 cm^{-1} lower than the TO1 mode. The strength of this mode strongly depends on the conditions under which it is calculated. We have used a finite displacements approach to calculate the force constant. For 0.025 Å displacement from their equilibrium position, the mode-plasma frequency $\sqrt{\Delta\varepsilon}\omega_{TO}$ of the new mode is about 270 cm^{-1} (for comparison the TO1 mode has the plasma frequency around 1040 cm^{-1}). If the displacement is only 0.0027 Å then the calculated mode-plasma frequency is only 24 cm^{-1}. This is a sort of probe of anharmonicity and it points to a rather strong anharmonicity of this particular mode. This mechanism of the mode activation requires a short-range magnetic order at least up to 150 K. A recent, not yet published, μSR experiment[42] performed on bulk $EuTiO_3$ revealed short-range magnetic correlations up to 300 K, which is rather surprising because the AFM critical temperature is only 5.3 K.

Finally, we can conclude that the new mode near 105 cm^{-1} is of the same symmetry as the TO1 mode. It probably stems from the lowest-frequency optical phonon branch and it is activated from the BZ edge due to the AFD phase transition. Its activation in IR spectra requires local reduction of the symmetry, which can occur due to creation of polar or magnetic nanoclusters.

VI. CONCLUSION

Due to the compressive strain, all polar phonons polarized in the plane of the $EuTiO_3$ films are considerably stiffened in comparison to the bulk ceramics. Below 150 K, a new IR active mode was revealed near 110 cm^{-1}. We understand it as optical phonon from the BZ edge, which activates in the IR spectra below the AFD phase transition under circumstance of the presence of polar and/or magnetic nanoclusters. Magnetization data show that the compressive strain enhances the Néel AFM temperature by 1 K due to the strain-enhanced superexchange interaction. IR reflectance studies in magnetic field revealed a striking tuning of the lowest phonon frequency with the magnetic field. This is responsible for the magnetodielectric effect reported previously in the bulk $EuTiO_3$.[11] Observed change of the polar phonon frequency

with the magnetic field is in agreement with our theoretical calculations. Similar IR experiments with magnetic field are rather rare in the literature because the phonon frequency changes are usually under spectral resolution in materials without a strong spin-phonon coupling. Our study shows that the IR reflectance measurements of a rather thin film can be more sensitive to the magnetic field (in the case of suitable nonconducting substrate) than the reflectivity spectra of the bulk samples or transmission spectra of the thin films. So, the IR reflectance spectroscopy is a very promising tool for a study of the magnetodielectric effect as well as of structural phase transitions in thin dielectric films deposited on electrodeless nonconducting substrates.

ACKNOWLEDGMENTS

This work was supported by the Czech Science Foundation (Projects No. 202/09/0682 and No. P204/12/1163). J. H. Lee and D. G. Schlom were supported by the National Science Foundation through the MRSEC program (Grant No. DMR-1120296). T. Birol and C. J. Fennie were supported by the DOE-BES under Grant No. DE-SCOO02334. Part of this work was supported by the Young Investigators Group Programme of the Helmholtz Association, Germany, Contract No. VH-NG-409. K.Z.R. and M.L. gratefully acknowledge the support of Jülich Supercomputing Centre. We are grateful to E. Šantavá for help with the magnetic measurements.

*kamba@fzu.cz

[1] K. F. Wang, J.-M. Liu, and Z. F. Ren, Adv. Phys. **58**, 321 (2009).
[2] C. J. Fennie and K. M. Rabe, Phys. Rev. Lett. **97**, 267602 (2006).
[3] J. H. Lee, L. Fang, E. Vlahos, X. Ke, Y. W. Jung, L. Fitting Kourkoutis, J. W. Kim, P. J. Ryan, T. Heeg, M. Roeckerath, V. Goian, M. Bernhagen, R. Uecker, P. C. Hammel, K. M. Rabe, S. Kamba, J. Schubert, J. W. Freeland, D. A. Muller, C. J. Fennie, P. E. Schiffer, V. Gopalan, E. Johnston-Halperin, and D. G. Schlom, Nature (London) **466**, 954 (2010); **476**, 114 (2011). Details about IR studies of $EuTiO_3/DyScO_3$ can be found in electronic supplement [http://www.nature.com/nature/journal/v466/n7309/extref/nature09331-s1.pdf].
[4] T. R. McGuire, M. W. Shafer, R. J. Joenk, H. A. Alperin, and S. J. Pickart, J. Appl. Phys. **37**, 981 (1966).
[5] K. Z. Rushchanskii, S. Kamba, V. Goian, P. Vaněk, M. Savinov, J. Prokleška, D. Nuzhnyy, K. Knížek, F. Laufek, S. Eckel, S. K. Lamoreaux, A. O. Sushkov, and M. Ležaić, Nat. Mater. **9**, 649 (2010).
[6] K. Z. Rushchanskii, N. A. Spaldin, and M. Ležaić, Phys. Rev. B. **85**, 104109 (2012).
[7] J. Brous, I. Fankuchen, and E. Banks, Acta Crystallogr. **6**, 67 (1953).
[8] A. Bussmann-Holder, J. Köhler, R. K. Kremer, and J. M. Law, Phys. Rev. B **83**, 212102 (2011).
[9] M. Allieta, M. Scavini, L. Spalek, V. Scagnoli, H. C. Walker, C. Panagopoulos, S. Saxena, T. Katsufuji, and C. Mazzoli, e-print arXiv:1111.0541.
[10] V. Goian, S. Kamba, O. Pacherova, J. Drahokoupil, F. Laufek, A. Fuith, W. Schranz, J. Prokleška, M. Kachlík, K. Maca, A. Shkabko, A. Weidenkaff, and J. Hlinka (unpublished).
[11] T. Katsufuji and H. Takagi, Phys. Rev. B **64**, 054415 (2001).
[12] V. V. Shvartsman, P. Borisov, W. Kleemann, S. Kamba, and T. Katsufuji, Phys. Rev. B **81**, 064426 (2010).
[13] S. Kamba, D. Nuzhnyy, P. Vaněk, M. Savinov, K. Knížek, Z. Shen, E. Šantavá, K. Maca, M. Sadowski, and J. Petzelt, Europhys. Lett. **80**, 27002 (2007).
[14] V. Goian, S. Kamba, J. Hlinka, P. Vaněk, A. A. Belik, T. Kolodizhnyi, and J. Petzelt, J. Eur. Phys. B **71**, 429 (2009).
[15] H. Akamatsu, Y. Kumagai, F. Oba, K. Fujita, H. Murakami, K. Tanaka, and I. Tanaka, Phys. Rev. B **83**, 214421 (2011).
[16] J. H. Lee, X. Ke, N. J. Podraza, L. Fitting Kourkoutis, T. Heeg, M. Roeckerath, J. W. Freeland, C. J. Fennie, J. Schubert, D. A. Muller, P. Schiffer, and D. G. Schlom, Appl. Phys. Lett. **94**, 212509 (2009).
[17] V. Železný, I. Fedorov, and J. Petzelt, Czech. J. Phys. **48**, 537 (1998).
[18] F. Gervais, in *Infrared and Millimeter Waves*, Vol. 8, edited by K. J. Button (Academic, New York, 1983), Chap. 7, p. 279.
[19] V. Bovtun, V. Pashkov, M. Kempa, S. Kamba, A. Eremenko, V. Molchanov, Y. Poplavko, Y. Yakymenko, J. H. Lee, and D. G. Schlom, J. Appl. Phys. **109**, 024106 (2011).
[20] T. Birol and C. J. Fennie (unpublished).
[21] K. Kugimiya, K. Fujita, K. Tanaka, and K. Hirao, J. Magn. Magn. Mater. **310**, 2268 (2007).
[22] K. Fujita, N. Wakasugi, S. Murai, Y. Zong, and K. Tanaka, Appl. Phys. Lett. **94**, 062512 (2009).
[23] J. Petzelt, G. V. Kozlov, and A. A. Volkov, Ferroelectrics **73**, 101 (1987).
[24] D. G. Schlom, L.-Q. Chen, Ch.-B. Eom, K. M. Rabe, S. K. Streiffer, and J.-M. Triscone, Annu. Rev. Mater. Res. **37**, 589 (2007).
[25] R. F. Schaufele, M. J. Weber, and B. D. Silverman, Phys. Lett. A **25**, 47 (1967).
[26] J. M. Worlock and P. A. Fleury, Phys. Rev. Lett. **19**, 1176 (1967).
[27] G. A. Samara and P. S. Peercy, *Solid State Physics, Advances in Research and Applications*, Vol. 36, edited by H. Ehrenreich, F. Seitz, and D. Turnbull (Academic New York, 1981), p. 1.
[28] T. Ruf, C. Thomsen, R. Liu, and M. Cardona, Phys. Rev. B **38**, 11985 (1988).
[29] A. B. Sushkov, J. L. Musfeldt, Y. J. Wang, R. M. Achey, and N. S. Dalal, Phys. Rev. B **66**, 144430 (2002).
[30] A. Pimenov, T. Rudolf, F. Mayr, A. Loidl, A. A. Mukhin, and A. M. Balbashov, Phys. Rev. B **74**, 100403(R) (2006).
[31] J. Cao, L. I. Vergara, J. L. Musfeldt, A. P. Litvinchuk, Y. J. Wang, S. Park, and S.-W. Cheong, Phys. Rev. Lett. **100**, 177205 (2008).
[32] I. Dzyaloshinskii, Philos. Mag. **89**, 2079 (2009).
[33] D. Nuzhnyy, J. Petzelt, S. Kamba, T. Yamada, M. Tyunina, A. K. Tagantsev, J. Levoska, and N. Setter, J. Electroceram. **22**, 297 (2009).
[34] J. H. Haeni *et al.*, Nature (London) **430**, 758 (2004).
[35] B. C. Chakoumakos, D. G. Schlom, M. Urbanik, and J. Luine, J. Appl. Phys. **83**, 1979 (1998).
[36] P. A. Fleury, J. F. Scott, and J. M. Worlock, Phys. Rev. Lett. **21**, 16 (1968).
[37] J. Petzelt *et al.*, Phys. Rev. B **64**, 184111 (2001).
[38] T. Ostapchuk *et al.*, Phys. Rev. B **66**, 235406 (2002).

[39]D. Nuzhnyy, J. Petzelt, S. Kamba, P. Kužel, C. Kadlec, V. Bovtun, M. Kempa, J. Schubert, C. M. Brooks, and D. G. Schlom, Appl. Phys. Lett. **95**, 232902 (2009).

[40]J. L. Bettis, M.-H. Whangbo, J. Köhler, A. Bussmann-Holder, and A. R. Bishop, Phys. Rev. B **84**, 184114 (2011).

[41]J. Hlinka, J. Petzelt, S. Kamba, D. Noujni, and T. Ostapchuk, Phase Transitions **79**, 41 (2006).

[42]A. Bussmann-Holder, Fundamental Physics of Ferroelectrics and Related Materials, 2012, Argonne, USA, January 29 - February 1, 2012 (private communication).